SciMedCentral

JSM Environmental Science & Ecology

Research Article

Statistical Analyses of Ambient Dose Equivalent Considering High Number of Realistic Flight Paths and Dynamic Ground Level Enhancement Model

Guillaume Hubert[1]* and Sebastien Aubry[2]

[1]*ONERA / DPHY, University of Toulouse, France*
[2]*ONERA / DTIS, University of Toulouse, France*

***Corresponding author**
Guillaume Hubert, ONERA / DPHY, University of Toulouse, 31055 Toulouse, France, Tel: 33-562252885; Fax: 33-5622252569; Email: guillaume.hubert@onera.fr

Submitted: 17 April 2018

Accepted: 15 May 2018

Published: 18 May 2018

ISSN: 2333-7141

Keywords

- Atmospheric ionizing radiation; Radiation exposure; Solar flare; Ground level enhancement; Statistical analyses

Abstract

The objective of this work is to investigate impacts of solar and galactic cosmic rays on flights by considering high realistic paths issued from Flight Plan updated with Radar Data. Models and approaches used were previously validated by comparison of calculated and measured ambient dose equivalents or cosmic ray variations during quiet solar activity and GLEs. Thus, to consider continents or sub-continents representative of European international air traffic, five flights were selected. They link Paris (France) to Los Angeles, New York (United States), Tokyo (Japan), Johannesburg (South Africa) and Sao Paulo (Brazil) city. Moreover, several hundred realistic paths are considered for each of these flights. The objective is to analyze statistically the ambient dose equivalents considering path characteristics and GLE/quiet scenario, and thus demonstrate the complexity to assess the real radiation exposure, particularly during solar event.

ABBREVIATIONS

ATMORAD: Atmospheric Radiation; SEP: Solar Energetic Particles; GCR: Galactic Cosmic Ray; SCR: Solar Cosmic Ray; CR: Cosmic Ray; ATMORAD: Atmospheric Radiation; NM: Neutron Monitor; GLE: ground Level Enhancement; GEANT4: Geometry and Tracking; LIS: Local Interstellar Spectrum; ICRP: International System of Radiological Protection

INTRODUCTION

Studies of the atmospheric ionizing radiations and their dynamics are required in many research and industrial fields. Spectra and/or fluxes are used to assess the human radiation effect [1,2] and to quantify the Single Event Effect (SEE) [3-11] risk in avionic. Other applications concern atmospheric muons which can be used to image the geological structure density [12-13], and recent applications demonstrate the method interest to monitor magma movements inside volcanoes [14] or density variations in aquifers. Thus, the interest to quantify the atmospheric ionizing radiations is essential, demanding to consider impacts of ground geophysical properties and space conditions (activity, solar flare, primary cosmic rays).

The interaction of primary cosmic rays with the nuclei of the constituents of the atmosphere induced secondary particles as neutrons, protons, muons etc., whose fluxes will vary according to the altitude, the latitude, the longitude and the space weather. Moreover, some mechanism or sources can also modify fluxes or energetic properties, especially for neutrons in the ground environment. Indeed, neutron fluxes can be impacted by the interaction of alpha particles emitted by radon [15], by the weather condition [16-18] or by seismic activities [19-20]. Besides, cosmic and terrestrial sources, atmospheric neutrons may be also be generated by lightning discharges [21-22].

Thus, Cosmic rays are considered as a major source of natural radiation exposure to humans, and particularly for flight altitudes. International agencies have established recommended dose limits for both workers and the general public for different types of activities including terrestrial and high altitude level. Thus, national or continental regulations have been adopted in many areas based on these recommendations. Concerning the ICRP, recommendations for annual effective dose are 20 mSv and 1 mSv averaged over a five year period for aircrews and for the public, respectively. They also recommended a 2 mSv limit on the accumulated dose over nine months of pregnancy. In the point of view of human health, the epidemiological investigations based on large national and international data of aircrew indicate no clear association of health outcomes with cosmic radiation exposure. However, studies devoted to chromosome translocations provide some evidence suggesting that aircrew show increased cytogenetic changes with longer lifetime flight experience [23]. Other works [24] show that the excess ultraviolet radiation is a probable cause of the increased melanoma risk.

Previous works [25,26] was devoted to demonstrate the

ability to assess impacts of solar and galactic cosmic rays on typical transatlantic flights. First comparisons of calculations and measurement during quiet solar activity and GLEs were relevant. Thus, results showed that dose values vary drastically with the route path (i.e. latitude, longitude altitude) and with the dynamic of the solar event with respect to the path. However, the path number considered in these analyses, although sufficient to evaluate calculation uncertainties or variabilities, was not sufficient to provide a statistical analysis. Indeed, the statistical approach is important because a given flight is characterized by a large number of possible routes inducing a varying sensitivity to radiation. This is particularly reinforced by considering extreme events.

The aim of the paper is to investigate statistically the radiation exposure during extreme solar events while considering dynamics, physical parameters and flight paths. These analyses can contribute to improve the understanding of issues related to the influence of radiation exposure on safety regulations for flight personal during GLE. Realistic paths are issued from Flight Plan updated with Radar Data (statistics considered in [25-26] were too weak to investigate this impact), and it integrates the path changes induced by the meteorological conditions or by the traffic regulation. Thus, to consider continents or sub-continents representative of European international air traffic, five flights were selected. They link Paris (France) to Los Angeles, New York (United States), Tokyo (Japan), Johannesburg (South Africa) and Sao Paulo (Brazil) city. Moreover, several hundred realistic paths are considered for each of these flights. The objective is to analyze statistically the ambient dose equivalents considering path characteristics and GLE/quiet scenario, and thus demonstrate the complexity to assess the real radiation exposure, particularly during solar event.

MATERIALS AND METHODS

Galactic and solar CR modeling for extensive air-shower simulations

To describe primary CR spectrum, the Force-Field approximation model is usually used. This model provides a simple parametric approximation of the differential spectrum of GCR and it contains only one variable parameter named the modulation potential φ(t). The sunspot number and φ(t) are particularly relevant at providing an overview of the solar activity. Thus, several methodologies have been developed for the reconstruction of time series of the modulation potential φ(t), as ATMORAD [28] based on GEANT4 simulations. Nevertheless, Solar Cosmic Ray (SCR) intensity distribution observed on the Earth depends on some characteristics as the source site, acceleration mechanism, coronal transport and ejection profile as well as the transport of accelerated particles through the interplanetary magnetic field.

During typical SEP events with enhanced flux of low energy particles (i.e. < 0.1 GeV for protons), the effect is limited to the upper atmosphere, and it is sufficient to apply an analytical approximation of direct ionization. The GCR modulation can be described thanks models, among which the Force-Field approximation which stipulates that the GCR Local Interstellar Spectrum (LIS) varies with the solar modulation potential expressed in GV. However, during a GLE, the solar proton spectrum can extend up to 1-10 GeV, energies that are high enough to induce cascades of particles in the atmosphere.

In [26], a GLE model was described and the SCR can be expressed in the equation (1).

$$S_{SCR}(E,t) = S(E,t) \times \Psi(\Omega,R,t)$$

Ψ(Ω,R,t) is the anisotropy function reflecting the distribution of solar cosmic ray particles at the top of the atmosphere during the solar event, revealing information on the way these particles propagated in the interplanetary magnetic field and finally arrived at the vicinity of the Earth. S(E,t) is the differential SCR rigidity spectrum in a solid angle of asymptotic direction. A model detailed in [27], proposed to express the differential SCR energy spectrum thanks to the equation (2):

$$S(E,t) = \frac{\delta J(E,t)}{\delta E}$$

J(E,t) is the integral omnidirectional integrated fluence of SEP and it can be represented using the Band function (Band 1993), presented in equation (3).

$$J(E,t) = J_0(E,t) \times \left(\sqrt{E^2 + 2.E_0.E}\right)^{-\gamma(t)}$$

J_0(E,t) is the solar energetic particle intensity, γ(t) is the power index and E_0 is the rest energy of proton. Thus considering these terms, the differential SCR energy spectrum can be described by the equation (4):

$$S(E,t) = \frac{J_0(t) \times \gamma(t)}{4.\pi} \times \left(\sqrt{E^2 + 2.E_0.E}\right)^{-\gamma(t)} \times \frac{E + E_0}{E^2 + 2.E_0.E}$$

The anisotropy function was investigated in [27] thanks to NMs data, and it was described by the anisotropy index characterizing the width of the solar particle beam.

Thus, during GLE, the incidental primary spectrum is composed by the GCR and SCR. The spectral fluence rate of secondary particles induced by extensive showers and taking into account the magnetic field impact can be calculated using ATMORAD simulations [28-30]. It integrates databases describing the atmospheric radiation and built thanks to simulations of extensive air showers. Databases were obtained using nuclear transport toolkit (GEANT4 [31], Corsika [32]).

The Force-Field approximation and GLE model on SCR description were coupled with air-shower descriptions, offering the opportunity to study the neutron spectral variations considering quiet, FD and/or GLE scenario. Modelling of GLE #5 and #69 were validated in previous works [26], they were preferentially used in this work.

Flight path database and ambient dose equivalent

Flight trajectories are based on the Eurocontrol Demand Data Repository (DDR [33]) and consider realistic flight plan with and without regulations or updated with Radar Data from CFMU (Central Flow Management Unit). These trajectories are

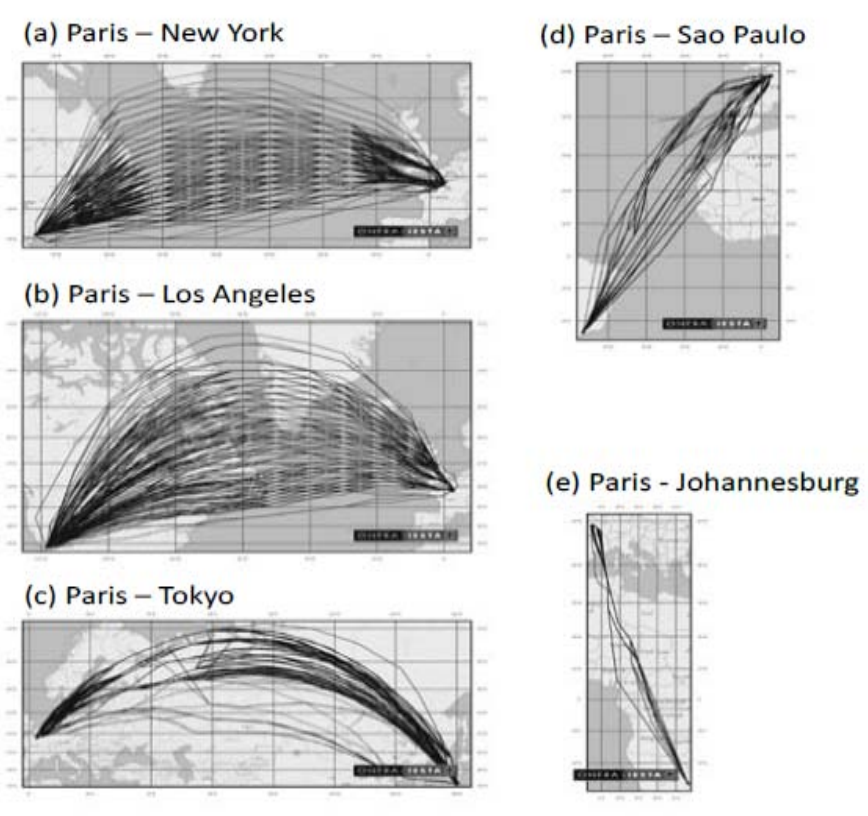

Figure 1 World maps of flight paths linking Paris to (a) New York, (b) Los Angeles, (c) Tokyo, (d) Sao Paulo and (e) Johannesburg.

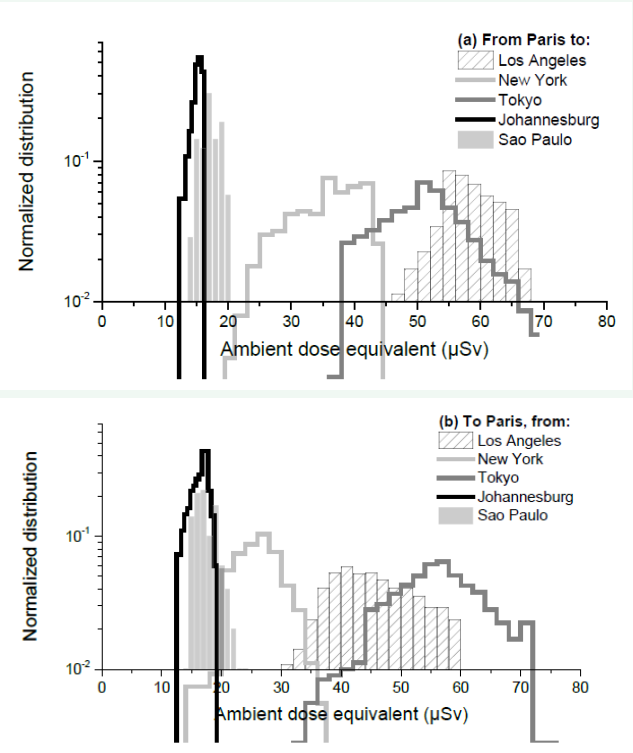

Figure 2 Normalized distribution of the Ambient dose equivalent during quiet solar activity (solar modulation of 700 MV) and for five selected flight routes characterized by high number of paths (Paris to Los Angeles, New York, Tokyo, Johannesburg and Sao Paulo city).

available in different states: 1) M1: from Flight Plan, 2) M2: M1 with regulations and 3) M3: Flight Plan updated with CFMU. The M3 data has been used here, in order to take into account the regulation actions and the air traffic control orders. Each path was characterized by geophysical locations (timing, longitude, latitude and altitude), airplane type, city of departure and arrival.

Five flights were selected considering high statistical path number issued from Flight Plan updated with Radar Data (CFMU, M3). To consider continents or sub-continents representative of European international air traffic, flights linking Paris to New York, Los Angeles, Tokyo, Sao Paulo and Johannesburg city are investigated, and several hundred trajectories are considered for each of these flights. Figure 1 presents a world mapping describing these flights. There is a great diversity of trajectories for a given flight; it is especially true for Los Angeles, New York and Tokyo city. Some anomalies are identifiable on the trajectory, which reflects flight plan modifications probably due to weather conditions. In the specific case of Paris - Tokyo flights, it is possible to distinguish flights using a Siberian route and flights using a low latitude route. A fairly similar remark can be made about Paris – Los Angeles flights.

Some works [34-35] demonstrated the shielding impacts to radiation levels, in particular aircraft structures and materials. Thus, the ambient dose equivalent can be different inside the aircraft depending on locations and quantity of material. This contribution will be taken into account in future works by introducing airplane description in transport simulations. This work focuses to GLE impact on dose assessments. Considering the previous descriptions, the ambient dose equivalent H^* for a given flight can be calculated using conversion coefficients $f_i^{H^*}$ [36-41] and thank to the following equation:

$$H^* = \sum_{i=n,p,\mu,e} \int_{path} \int_{E} \frac{\partial \varphi_i(E,t)}{\partial E} f_i^{H^*}(E) \delta E \delta_{path}$$

The GLE model was applied during extreme events occurring on the 23 February 1956 (#5) and the 20 January 2005 (#69), respectively. Besides the differential SCR rigidity spectrum and due to the anisotropy characteristics, the ambient dose equivalent depends on the dynamic. Contrary to the Forbush decrease, GLE are prompt events which complicate the dose assessment. Indeed, dose values vary drastically with the route profile but also with the phasing of the solar event.

RESULTS AND DISCUSSION

Statistical analyses applied to selected flights

Figure 2 presents normalized distribution distributions of the ambient dose equivalent during quiet solar activity (i.e. solar modulation of 700 MV) and for the five selected flights. Figure 2a concerns flights from Paris and Figure 2b flights to Paris. This distinction is important because the flight durations are not the same due to the prevailing atmospheric currents (East - West), and the air corridors (in the point of view of latitude relatively unaffected by the flight direction.

Statistical analyses applied to selected flights during GLE

Same analyses were performed considering the GLE #69 occurred 4 hours after the departure of flights (Figure 3-Figure 5), for Los Angeles, New York and Tokyo flights. Moreover, results presented in Figure 3 to 5 allow investigating the impact of the direction (East-West or West-East, i.e. from or to Paris).

Then, it is interesting to note a significant impact of direction in ambient dose distributions for all selected flights, particularly during GLE. This confirms the interest of accurately taking into account the dynamics of GLE in the dose assessment.

For Paris – Tokyo flights (Figure 5), normalized distributions are from 50 to 280 μSv for the East-West (EW) direction, while the range is from 125 to 360 μSv for the West-Est (WE) direction. In other words, there may be a factor up to 5 on the ambient dose level induced by the path. The data comparison shows that some paths are weakly sensitive to the impact of the GLE. This suggests that during extreme events, it should be possible to reroute the airplane to avoid the radiation impacts. However, in the case of GLEs for which the solar particles are quasi-relativistic, it is not easy to anticipate this problematic for current air traffic. Conversely, it is possible to issue recommendations to avoid certain geographic regions or latitudes

In the specific case of Paris – Johannesburg and Paris – Sao Paulo flights, the GLE impact on ambient dose levels is relatively limited, with an increase of up to 20%. This is primarily an effect of latitude since these routes cross the tropical and equatorial latitudes.

Figure 6 presents the average value of ambient dose equivalent calculated on selected flights, using realistic sampling of routes and considering the both GLE. Ambient dose equivalents obtained during quiet period is also presented (solar modulation of 700 MV). The first analysis concerns the average ambient dose equivalent obtained during quiet solar activity. Despite the directions of the flight route, results are quite homogeneous for certain flights. For example Paris to Sao Paulo for which the dose is in the order of 17 μSv. The main reason is that the departure and the arrival latitudes are quite similar. This is a finding that mainly concerns North-South routes because they undergo the same atmospheric currents. In all other cases, differences are observed in the average values. The route analysis confirms that air corridors and altitudes are mapped according to the direction of flight, which is a consequence of air regulations.

Focusing on the results obtained with GLEs, a very large asymmetry is observed for some flight routes, the most spectacular example concerning Los Angeles and Tokyo flights. Indeed, considering Paris – Tokyo flights and GLE #5, the average ambient dose equivalent values are 1146 and 420 μSv in the WE and EW directions, respectively. Moreover, results confirm that North-South routes are characterized by a relatively low dissymmetry, even during a GLE.

The worst radiation exposure level was obtained for the Paris – Los Angeles flight and considering the GLE #5, i.e. in the order of 1.7 mSv. In comparison to the recommended limit of 2 mSv on the accumulated dose over nine months required by the ICRP, it seems obvious that a realistic assessment is required to comply with the regulations. In other terms, this assessment is relevant if it integrates realistic descriptions of path and physical properties of GLE. Moreover, the problematic concerns the regulation defined for the passengers and consideration should be given to this very topical issue due to the regular use of air transport.

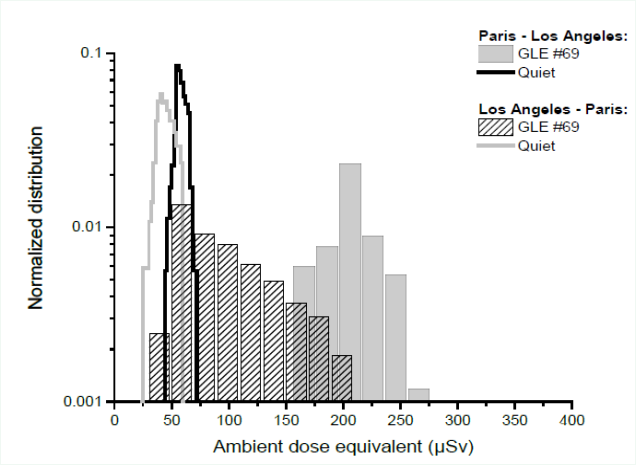

Figure 3 Normalized distribution of the Ambient dose equivalent considering the quiet solar activity (solar modulation of 700 MV) and the GLE #69 occurring 4 hours after the flight departure. Results concern the Paris – Los Angeles and Los Angeles – Paris flights and are based on high number of paths.

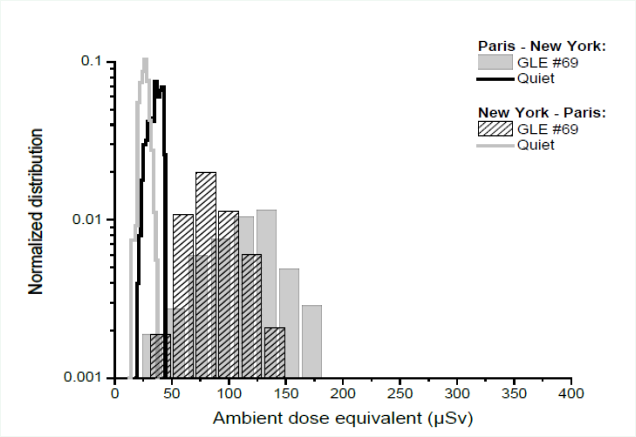

Figure 4 Normalized distribution of the Ambient dose equivalent considering the quiet solar activity (solar modulation of 700 MV) and the GLE #69 occurring 4 hours after the flight departure. Results concern the Paris – New York and New York – Paris flights and are based on high number of paths.

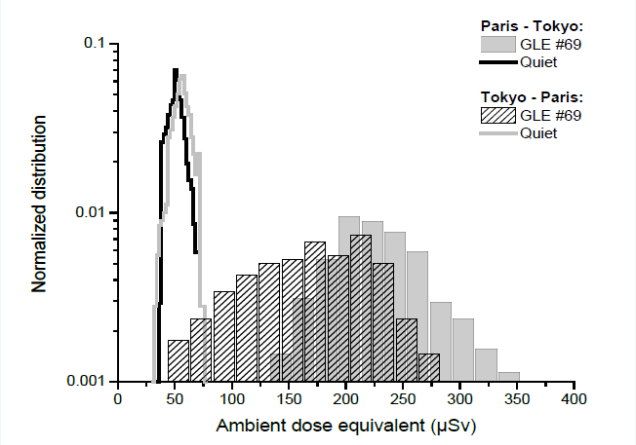

Figure 5 Normalized distribution of the Ambient dose equivalent considering the quiet solar activity (solar modulation of 700 MV) and the GLE #69 occurring 4 hours after the flight departure. Results concern the Paris – Tokyo and Tokyo – Paris flights and are based on high number of paths.

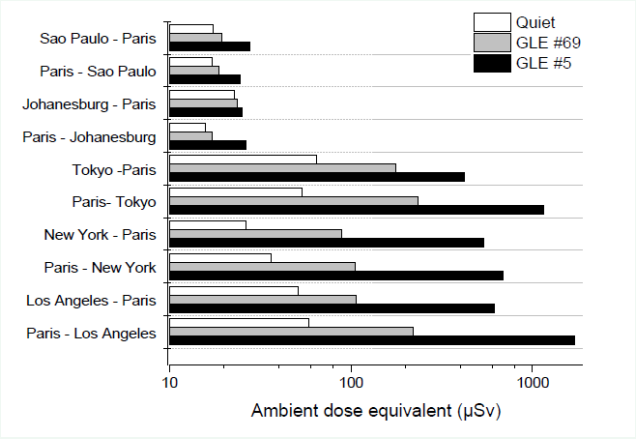

Figure 6 Average value of ambient dose equivalent (μSv) obtained for selected flights, considering the quiet period, GLE #69 and #5 occurring 4 hours later departure.

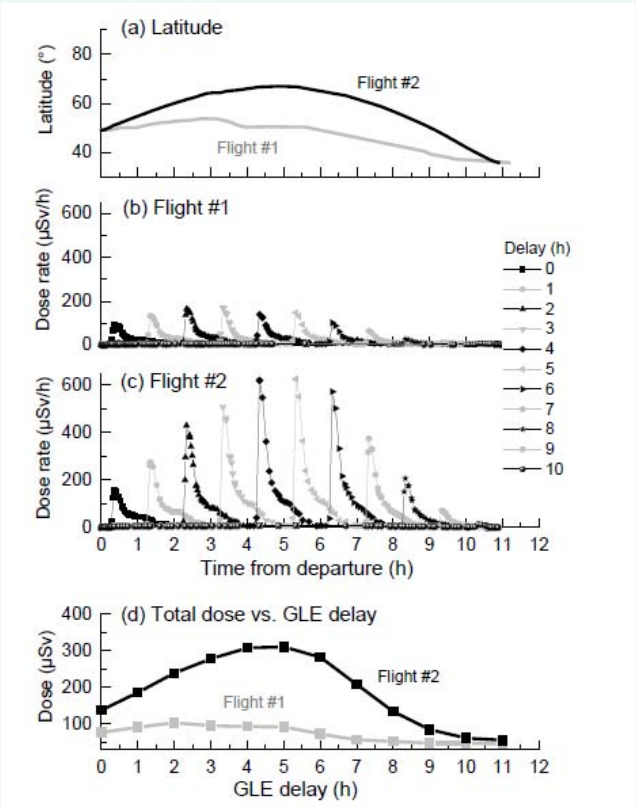

Figure 7 (a) Paris-Tokyo flight route (#1 and #2), dynamics of the dose rate for flights #1 (b) and #2 (c) considering the GLE #69 scenario for several occurrence delays (from 0 to 11 h). Total ambient dose equivalents versus GLE delay (from 0 to 10 h) are presented in (d).

Impact of the GLE time occurrence

The time defining the GLE occurrence has an importance in the assessment of the ambient dose equivalent. Two Paris – Tokyo flights were selected to investigate the impact of GLE occurrence time, the first one being the lowest dose (quiet period), while the second induced the highest dose. Figure 7a presents latitude dynamics of flights #1 and #2. The route #2 crosses latitude of 70° while the second does not reach 52°. Moreover, it is important to specify that altitude dynamics are quite similar as well as flight duration (11.7 km and 11 h, respectively)

Then, Figure 7b and Figure 7c show estimates for the total dose rate profiles (in μS/h) during both flights and considering the GLE #69 scenario occurring later the flight departure. The delay of the GLE occurrence varies from 0 to 11 h. A significant difference is observed between these flights, whatever the delay. It is obvious that this difference is the consequence of the flight

latitude. A factor of 3.5 is observed by comparison of dose rate amplitudes of flights (considering the same delay). Finally, this analysis shows that according to the dynamic phasing of the GLE and according to the path characteristics, the dose rate can vary up to a factor 10, involving drill variation of the total ambient dose equivalent. It is therefore difficult to assert the dose level induced by a GLE without considering a physical and dynamic description.

The total ambient dose equivalents as function of the delay are presented in Figure 7d for the both flights. The ratios between the two flights range from a factor of 1.8 to a factor of 4. For delays of 9 or more, there is no difference in the total ambient dose equivalent, which may be directly related to the flight latitude (typically inferior to 45°) for which the GLE has a non-significant effect.

CONCLUSION

To investigate the ambient dose equivalent during quiet solar activity and extreme solar events (GLE), realistic paths for five selected flights representative to the European international air traffic were considered. There would be an interest in considering a greater number of flights, or considering database describing global air traffic over a significant period. This will be the subject of future work.

Previous works [25-26] had shown the validity of the physical models used in these analyzes, during quiet solar periods (dose measurements and calculations) and also during GLEs based on the cosmic ray variations issued from neutrons monitors.

Statistical analyses show that ambient dose equivalents vary drastically with the route path (latitude, longitude and altitude) and with the phasing of the solar event. Indeed, GLE are prompt events which complicate the dose assessment. Results show that contrarily to the classical solar flare inducing Forbuch decreases or classical GLEs, severe GLEs can induce much larger dose levels that it is very complicated to assess. Additional doses induced by an extreme solar event can impact significantly the annual effective dose, for aircrews but also for passengers whose flying frequencies can be extremely high. This extra dose level depends on several physical parameters, i.e. the differential SCR rigidity spectrum, the anisotropy function reflecting the distribution of SCR particles at the top of the atmosphere during the solar event, and their dynamics. As mentioned in the introduction, the recommendations for annual effective dose are of 1 mSv (over a five year period). Orders of magnitude illustrate the importance of considering more refined physical approach to obtain reliable calculation of dose levels.

REFERENCES

1. Reitz G. Radiation environment in the stratosphere. Radiat Prot Dosimetry. 1993; 48: 5-20.
2. Goldhagen, Clem J, Wilson JW. The energy spectrum of Cosmic-Ray induced Neutrons measured on an Airplane over a wide range of Altitude and Latitude. Radiat Prot Dosimetry. 2004; 110: 387-392.
3. Peronnard P, Velazco R, Hubert G, Federico C, Cheminet A, Silva-Cardenas, et al. Real-life SEU experiments on 90nm SRAMs in Atmospheric Environment: measures vs. predictions done by means of MUSCA SEP3 platform. IEEE TNS. 2009.
4. Raine M, Hubert G, Paillet P, Gaillardin M, Bournel A. Implementing Realistic Heavy Ion Tracks in a SEE Prediction Tool: Comparison Between Different Approaches. Nucl Sci. 2012; 59: 950-957.
5. Hubert G, Artola L, Regis D. Impact of scaling on the soft error sensitivity of bulk, FDSOI and FinFET technologies due to atmospheric radiation. VLSI. 2015; 50: 39-47.
6. Lambert D, Baggio J, Hubert G, Ferlet-Cavrois V, Flament O. Neutron-induced SEU in SRAMs: Simulations with n-Si and n-O interactions. Nucl Sci. 2005; 52: 2332-2339.
7. Lambert D, Baggio J, Hubert G, Paillet P, Girard S, Saigne F. Analysis of Quasi-Monoenergetic Neutron and Proton SEU Cross Sections for Terrestrial Applications. Nucl Sci. 2006; 53: 1890-1896.
8. Hubert G, Velazco R, Frederico C, Cheminet A, Silva-Cardenas C, Caldas LVE, et al. Continuous high-altitude measurements of cosmic ray neutron and SEU/MCU at various locations: correlation and analyses based-on MUSCA-SEP^3. Nucl Sci. 2013; 60: 2418-2426.
9. Hubert G, Bougerol A, Miller F, Buard N, Anghel L, Carriere T, et al. Prediction of transient induced by neutron/proton in CMOS combinational logic cells. Proceedings of the 12th IEEE International On-Line Testing Symposium. 2006; 63-71.
10. Artola L, Gaillardin M, Hubert G, Raine M, Paillet P. Modeling Single Event Transients in Advanced Devices and ICs. IEEE Trans Nucl Sci. 2015; 62: 1528-1539,
11. Toure G, Guillaume Hubert, Karine Castellani-Coulie, Sophie Duzellier, Jean-Michel Portal. Simulation of Single and Multi-Node Collection: Impact on SEU Occurrence in Nanometric SRAM Cell. IEEE Trans Nucl Sci. 2011; 58: 862-869.
12. George EP. Cosmic rays measure overburden of tunnel. Commonwealth Engineer. 1955; 455–457.
13. Alvarez L, Anderson JA, Bedwei FA, Burkhard J, Fakhary A, Giris A, et al. Search for hidden chambers in the pyramids. Sci. 1970; 167: 832–839.
14. Tanaka H, Nagamine K, Nakamura SN, Ishida K, Kawamura N, Shimomura K, et al. Development of the cosmic-ray muon detection system for probing internal-structure of a volcano. Hyperfine Interact. 2001; 138: 521-526.
15. Kuzhevskij BM, Nechaev OY, Panasyu MI, Sigaeva EA, Volodichev NN, Zakharov VA. Neutron field of the Earth: Origin and dynamics. J Korean Assoc Radiat Prot. 2001; 26: 315-319.
16. Eroshenko EP, Velinov A, Belov V, Yanke E, Pletnikov Y, Tassev Y, et al, editors. Relationships between cosmic ray neutron flux and rain flows. Proceedings of the 21st European Cosmic Ray Symposium, Tech. Univ. of Kosice, Kosice, Slovakia.
17. Lockwood JA, Yingst HE. Correlation of meteorological parameters with cosmic ray intensities. Phys Rev. 1956; 104: 1718-1722.
18. Mishev, Stamenov J, editors. Tendency for relation between rain flows and neutron flux at basic environmental observatory Moussala. Proceedings of the 21st European Cosmic Ray Symposium. Kosice, Slovakia, 2008.
19. Volodichev NN, Zakharov VA, Kuzhevskij BM, Nechaev OY, Podorolski AN, Chubenko AP, et al. editors. The flows of neutrons of space radiation and from terrestrial crust. Proceedings of the 27th International Cosmic Ray Conference. Hamburg, Germany, 2001.
20. Alekseenko VV, Djapuev DD, Gavriluk YM, Gromushkin DM, Kudjaev AU, Kuzminov VV, et al. editors. Observation of thermal neutron flux variations connected with lunar periods. Proceedings of the 30th International Cosmic Ray Conference, Mérida, Mexico, 2007.
21. Libby LM, Lukens HR. Production of radiocarbon in tree rings by lightning bolts. J Geophys Res. 1973: 78: 5902-5903.

22. Martin M, Alves MA. Observation of a possible neutron burst associated with a lightning discharge. J Geophys Res. 2010; 115: 1-4.

23. Zeeb H, Hammer G, Blettner M. Epidemiological investigations of aircrew: an occupational group with low-level cosmic radiation exposure. J Radiol Prot. 2012; 32: 15-19.

24. Hammer GP, Blettner M, Zeeb H. Epidemiological studies of cancer in aircrew. Radiat Prot Dosimetry. 2009; 136: 232-239.

25. Hubert G, Aubry S. Analysis of Solar and Galactic Cosmic Rays induced Atmospheric Ionizing Radiation: Impacts for typical transatlantic flights and Antarctica Environment. JSM Environ Sci Ecol. 2017; 5.

26. Hubert G, Aubry S. Atmospheric Cosmic-Ray Variation and Ambient Dose Equivalent Assessments Considering Ground Level Enhancement Thanks to Coupled Anisotropic Solar Cosmic Ray and Extensive Air Shower Modeling. Radiat Res. 2017; 188: 517-531.

27. Plainaki C, Belov A, Eroshenko E, Mavromichalaki H, Yanke V. Modeling ground level enhancements: Event of 20 January 2005. J Geophys Res. 2007; 112; 1-16.

28. Hubert G, Cheminet A. Radiation effects investigations based on atmospheric radiation model (ATMORAD) considering GEANT4 simulations of extensive air showers and solar modulation potential. Radiat Res. 2015; 184: 83-94.

29. Hubert G, Federico C, Pazianotto M, Gonzales O. Long and short-term atmospheric radiation analyses based on coupled measurements at high altitude remote stations and extensive air shower modeling. Astroparticle Physics. 2016; 74: 27-36.

30. Hubert G. Analyses of cosmic ray induced-neutron based on spectrometers operated simultaneously at mid-latitude and Antarctica high-altitude stations during quiet solar activity. Astroparticle Physics. 2016; 83; 30-39.

31. Agostinelli S, Allisonas J, Amako K, Apostolakis J, Araujo H, Arce P, et al. GEANT4-a simulation toolkit. Nucl Instr Meth Phys Res Sec A. 2003; 506; 250-303.

32. Corsika.

33. DDR, Euricontrol Demand Data Repository.

34. Ferrari, Pelliccioni M, Villari R. Evaluation of the influence of aircraft shielding on the aircrew exposure through an aircraft mathematical model. Radiat Prot Dosimetry. 2004; 108: 91-105.

35. Ferrari, Pelliccioni M, Villari R. A mathematical model of aircraft for evaluating the effects of shielding structure on aircrew exposure. Radiat Prot Dosimetry. 2005; 116: 331-335.

36. Pelliccioni M. Overview of Fluence-to-Effective Dose and Fluence-to-Ambient Dose Equivalent Conversion Coefficients for High Energy Radiation Calculated Using the FLUKA Code. Radiat Prot Dosimetry. 2000; 88: 279-297.

37. Ferrari A, Pelliccioni M, Pillon M. Fluence to Effective Dose Conversion Coefficients for Muons. Radiat Prot Dosimetry. 1997; 74: 227-233.

38. Ferrari A, Pelliccioni M, Pillon M. Fluence to Effective Dose and Effective Dose Equivalent Conversion Coefficients for Protons from 5 MeV to 10 GeV. Radiat Prot Dosimetry. 1997; 71: 85-91.

39. Ferrari A, Pelliccioni M, Pillon M. Fluence to Effective Dose and Effective Dose Equivalent Conversion Coefficients for Electrons from 5 MeV to 10 GeV. Radiat Prot Dosimetry. 1997; 71: 97-104.

40. Sato T, Endo A, Zankl M, Petoussi-Hens N, Niita K. Fluence-to-dose conversion coefficients for neutrons and protons calculated using the PHITS code and ICRP/ICRU adult reference for computational phantoms. Physics Med Biol. 2007; 54: 1997-2014.

41. Tatsuhiko S, Akira E, Koji N. Fluence-to-Dose Conversion Coefficients for Muons and Pions Calculated Based on ICRP Publication 103 Using the PHITS Code. Progress Nucl Sci Technol. 2011; 2: 432-436.

Cite this article

Hubert G, Aubry S (2018) Statistical Analyses of Ambient Dose Equivalent Considering High Number of Realistic Flight Paths and Dynamic Ground Level Enhancement Model. JSM Environ Sci Ecol 6(1): 1061.